International Journal of Advanced Smart Convergence Vol.9 No.4 156-166 (2020)
http://dx.doi.org/10.7236/IJASC.2020.9.4.156

IJASC 20-4-20

Machine-Learning-Based User Group and Beam Selection for Coordinated Millimeter-wave Systems

Sang-Lim Ju,[1] Nam-il Kim[2], Kyung-Seok Kim[3]

[1]*Doctor, Department of radio and communication engineering, Chungbuk National University, Korea*
[2]*Doctor, Telecommunications & Media Research Laboratory, Electronics and Telecommunications Research Institute, Korea*
[3]*Professor, Department of information and communication engineering, Chungbuk National University, Korea*
[1]*imaward@naver.com*, [2]*namilk@etri.re.kr*, [3]*kseokkim@chungbuk.ac.kr*

Abstract

In this paper, to improve spectral efficiency and mitigate interference in coordinated millimeter-wave systems, we proposes an optimal user group and beam selection scheme. The proposed scheme improves spectral efficiency by mitigating intra- and inter-cell interferences (ICI). By examining the effective channel capacity for all possible user combinations, user combinations and beams with minimized ICI can be selected. However, implementing this in a dense environment of cells and users requires highly complex computational abilities, which we have investigated applying multiclass classifiers based on machine learning. Compared with the conventional scheme, the numerical results show that our proposed scheme can achieve near-optimal performance, making it an attractive option for these systems.

Keywords: *Coordinated beamforming, Data-Driven learning, Machine-learning, Millimeter-wave, Ultra-dense network*

1. Introduction

Recently, mobile wireless communication (MWC) has gained attention as a general technology for the Fourth Industrial Revolution, and it is used in services such as manufacturing, healthcare, and automotive applications. The number of mobile Internet of Things connected devices is expected to reach 4.1 billion by 2024 [1]. To satisfy future requirements for advanced MWC, capabilities such as enhanced mobile broadband, massive machine-type communications, and low latency must be guaranteed. Thus, key technologies such as millimeter-wave (mmWave) [2] and small cell [3] have been considered for advancing MWC. Dense small cell networks are deployed because of the mmWave propagation characteristics, causing overlaps to appear between cells. In this case, intra- and inter-cell interferences (ICI) increase, and the system performance deteriorates [4]. Generally, user scheduling and beamforming are effective techniques for mitigating ICI while

Manuscript Received: November. 15, 2020 / Revised: November. 19, 2020 / Accepted: November. 28, 2020
Corresponding Author: kseokkim@chungbuk.ac.kr (Kyung-Seok Kim)
Tel: +82-10-8802-5823
Professor, Department of information and communication engineering, Chungbuk National University, Korea

improving spectral efficiency [5]-[8]. In [6]-[7], a joint scheme for user scheduling and beam selection based on precoder design was investigated in single-cell networks. Further, [8] explored greedy-search-based user scheduling to reduce computational complexity in an interference-limited environment. Additionally, to maximize the sum-rate of the multiple-input-multiple-output interference broadcast channel, the user scheduling based on branch-and-bound and a low-complexity semi-distributed scheme is studied in [9]. In [10], the beam and the user selection by taking into account highly correlated user channels is designed to maximize the sum data rate.

For advanced MWC, both fast processing and optimal performance must be achieved. Machine learning (ML), which has shown potential in various fields including MWC, offers a powerful solution. Most of the previous studies on MWC systems using ML aim to improve the spectral efficiency by selecting beams quickly and accurately [11]-[12]. However, mitigating ICI should be investigated to achieve the optimal performance of multicell systems for advanced MWC.

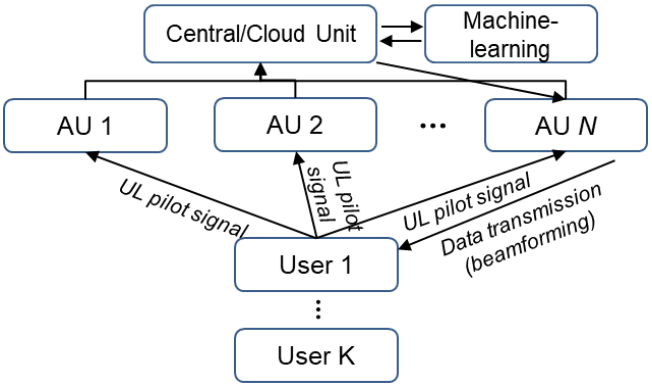

Figure 1. A block diagram of the proposed coordinated mmWave system in multicell network.

In this paper, we propose an optimal user group and radio frequency (RF) beam selection scheme based on exhaustive search for coordinated mmWave systems. In our proposed scheme, users are grouped, and groups and beams are then selected to maximize effective channel capacity to subsequently maximize spectral efficiency and mitigate ICI. Additionally, a near-optimal scheme that uses ML to minimize search time is proposed. Numerical results demonstrate that the proposed schemes can achieve better system performance than the conventional scheme.

2. System model

Consider a coordinated mmWave system in multicell network containing N small cells and N access units (AU)s with a uniform rectangular array of $N_t = N_v \times N_h$ antennas) which are assumed to be connected to a cloud processing unit (CU) as shown in Fig 1. K single antenna users are deployed in N small cells. N_v and N_h are the number of antennas in the vertical and horizontal directions, respectively. Small cells are uniformly deployed in an urban microcell. Users are assumed to be located in an area where N small cells overlap, and the coordinated multipoint joint transmission is not considered. AUs receive user uplink pilot signals, and user scheduling and precoding for downlink transmissions are processed at the CU; uplink feedback is not required. Suppose that *n*th AU covers some user group $K_n = [1, \dots, |K_n|]$ and U_{k_n} denotes the kth user covered by nth AU, i.e. $U_{k_n} \in K_n$. The $N_t \times N$ mmWave channel matrix from N AUs to U_{k_n} is

$$\boldsymbol{H}_{k_n} = \left[\boldsymbol{H}_{k_n,1}, \ldots, \boldsymbol{H}_{k_n,N}\right], \tag{1}$$

where $\boldsymbol{H}_{k_n,m} \in \mathbb{C}^{1\times N_t}$ is the channel matrix from mth AU to U_{k_n}. The modeled channel in an urban microcell scenario is applied in [13]. On the downlink, a CU applies a $N_t \times K$ RF beamformer, $\boldsymbol{F}_{RF} = \left[f^{RF}_{1_{\hat{1}}}, \ldots, \boldsymbol{f}^{RF}_{|K_{\hat{1}}|}, \ldots, \boldsymbol{f}^{RF}_{|K_{\hat{N}}|}\right]$, $\hat{1}, \ldots, \hat{N} \in N$, where $\hat{1}, \ldots, \hat{N}$ denote indices of active cells. A $K \times K$ digital beamformer, $\boldsymbol{F}_D = [\boldsymbol{f}^D_1, \boldsymbol{f}^D_2, \ \ldots, \boldsymbol{f}^D_K]$. For simplicity, the hybrid beamformer $\boldsymbol{\mathcal{F}}_B \in \mathbb{C}^{N_t\times K}$ is expressed as

$$\boldsymbol{\mathcal{F}}_B = \boldsymbol{F}_{RF}\boldsymbol{F}_D = \left[\boldsymbol{\mathcal{f}}^B_{1_{\hat{1}}}, \ldots, \boldsymbol{\mathcal{f}}^B_{|K_{\hat{1}}|}, \ldots, \boldsymbol{\mathcal{f}}^B_{|K_{\hat{N}}|}\right]. \tag{2}$$

The received signal of U_{k_n} is denoted as y_{k_n} and written as

$$y_{k_n} = \boldsymbol{H}_{k_n,n}\sum_{k_n=1}^{|K_n|}\boldsymbol{\mathcal{f}}^B_{k_n}x_{k_n} + \sum_{j=1,j\neq n}^{N}\boldsymbol{H}_{k_n,j}\sum_{m_j=1}^{|K_j|}\boldsymbol{\mathcal{f}}^B_{m_j}x_{m_j} + \eta_{k_n}, \tag{3}$$

where first term represents the desired signal and the intra-cell interference, and the second term represents inter-cell interference from other AUs. In addition, x_{k_n} is the transmit symbol, $E\left\{\left\|x_{k_n}\right\|^2\right\} = 1$, and $\eta_{k_n} \sim N_{\mathbb{C}}(0,\sigma^2)$ is the noise vector.

Given the mmWave channel $\boldsymbol{H}_{k_n,n}$, and employing the hybrid beamformer $\boldsymbol{\mathcal{F}}_B$, the user U_{k_n} sum rate is

$$R_k = log_2\left(1 + \frac{\rho_k\left|\boldsymbol{H}_{k_n,n}\boldsymbol{\mathcal{f}}^B_{k_n}\right|^2}{1+\left(\sum_{j=1}^{N}\sum_{u_j=1}^{|K_j|}\rho_u\left|\boldsymbol{H}_{k_j,j}\boldsymbol{\mathcal{f}}^B_{u_j}\right|^2 - \rho_k\left|\boldsymbol{H}_{k_n,n}\boldsymbol{\mathcal{f}}^B_{k_n}\right|^2\right)}\right), \tag{4}$$

where ρ_k denotes the received signal-to-noise ratio (SNR) for *k*th user. The spectral efficiency R_S of the system is then calculated as

$$R_S = \sum_{k=1}^{K} R_k. \tag{5}$$

3. User-Group and Beam Selection

The main objective of this work is to provide an approach for selecting the optimal user group and RF beams that maximize spectral efficiency and mitigate ICI for advanced MWC. First, we propose a scheme that groups users and selects the optimal group and RF beams via an exhaustive search for all user groups. Second, a machine-learning-based scheme is proposed to reduce the computation time to enable application in practical fields, including ultradense networks.

3.1 Conventional Scheme Overview

In the systems with conventional selection methods, a CU or users select the optimal serving cell and RF beam without user grouping. The conventional approaches are widely used in current systems with downlink channel state information - reference signal, such as 4G or primary 5G. The high feedback overhead is required for large-scale antenna systems.

Perfect channel knowledge is assumed, the channel $\boldsymbol{H} \in \mathbb{C}^{N_t\times K\times N}$ is

$$\boldsymbol{H} = \begin{bmatrix} \boldsymbol{H}_{1,1} & \cdots & \boldsymbol{H}_{1,n} & \cdots & \boldsymbol{H}_{1,N} \\ & & \vdots & & \\ \boldsymbol{H}_{k,1} & \cdots & \boldsymbol{H}_{k,n} & \cdots & \boldsymbol{H}_{k,N} \\ & & \vdots & & \\ \boldsymbol{H}_{K,1} & \cdots & \boldsymbol{H}_{K,n} & \cdots & \boldsymbol{H}_{K,N} \end{bmatrix}, \tag{6}$$

where $\boldsymbol{H}_{k,n} \in \mathbb{C}^{1\times N_t}$ is the channel matrix from nth AU to kth user. The optimal serving cell n^*_k and RF

beam $w_{i_k^*}$ for kth user are determined by exhaustive search as

$$\{n_k^*, \boldsymbol{w}_{i_k^*}\} = arg \max_{\substack{w_i \in W \\ n \in N}} \|\boldsymbol{H}_{k,n}\boldsymbol{w}_i\|^2, \tag{7}$$

where $\boldsymbol{H}_{k,n_k^*} = \boldsymbol{H}_{k_{n_k^*},n_k^*}$ and $i = 1,\ldots,2^{B_c}$. B_c is the bit of the RF beamforming codebook, $\boldsymbol{W} = [\boldsymbol{w}_1, \boldsymbol{w}_2, \ \ldots, \boldsymbol{w}_{2^{B_c}}]$. $\boldsymbol{W}$ is generated by a Kronecker-product of two discrete Fourier transform codebooks [14]. An RF beamforming codeword $\boldsymbol{w}_i$ is $\boldsymbol{w}_i = \boldsymbol{w}_j^v \otimes \boldsymbol{w}_\ell^h$, and $\boldsymbol{w}_j^v$ and $\boldsymbol{w}_\ell^h$ are

$$\boldsymbol{w}_j^v = \frac{1}{N_v}\left[1, e^{-j\phi(j)}, \ldots, e^{-j\phi(j)(N_v-1)}\right], \tag{8}$$

$$\boldsymbol{w}_\ell^h = \frac{1}{N_h}\left[1, e^{-j\theta(\ell)}, \ldots, e^{-j\theta(\ell)N_h-1}\right], \tag{9}$$

where $j = 0,1,\ldots,2^{\frac{B_c}{2}} - 1$, $\ell = 0,1,\ldots,2^{\frac{B_c}{2}} - 1$. $\phi(j) = \frac{2\pi j}{2^{B_c/2}}$ and $\theta(\ell) = \frac{2\pi\ell}{2^{B_c/2}}$ denote the zenith and azimuth angles of departure, respectively. In (7), an RF beamforming vector $\boldsymbol{w}_{i_k^*}$ from n_k^*th AU is selected for kth user. The digital beamforming vector $\boldsymbol{f}_k^D$ is designed by zero-forcing of the effective channel:

$$\bar{\boldsymbol{H}}_k = \boldsymbol{H}_{k,n_k^*}\boldsymbol{F}_{RF}, \ \bar{\boldsymbol{H}}_k \in \mathbb{C}^{1\times K}, \tag{10}$$

$$\bar{\boldsymbol{H}} = [\bar{\boldsymbol{H}}_1, \ldots, \bar{\boldsymbol{H}}_K], \ \bar{\boldsymbol{H}} \in \mathbb{C}^{K\times K}, \tag{11}$$

where $\bar{\boldsymbol{H}}_k$ denotes the effective channel for kth user. The digital beamformer $\boldsymbol{V}$ is given by zero-forcing $\bar{\boldsymbol{H}}$ as $\boldsymbol{V} = \bar{\boldsymbol{H}}^H(\bar{\boldsymbol{H}}\bar{\boldsymbol{H}}^H)^{-1}$, and $\boldsymbol{f}_k^D$ is normalized as $\boldsymbol{f}_k^D = \boldsymbol{V}_k/\sqrt{(\boldsymbol{F}_{RF}\boldsymbol{V}_k)^H(\boldsymbol{F}_{RF}\boldsymbol{V}_k)}$.

3.2 Proposed Optimal User Group and Beam Selection

To maximize the spectral efficiency of a coordinated multicell mmWave system, the ICI must be considered, as in (3) and (4), in addition to selecting the optimal beam. Thus, the system performance depends strongly on the AU that selects the users to be covered. However, the ICI is not considered in the conventional scheme. As shown in (10), the effective channel is determined by the channel and RF beam between each AU and its covered user, so its gain provides a handle for improving the spectral efficiency and mitigating the ICI. Since each user is covered by an AU, a $K \times 1$ channel link must be selected among the $K \times N$ channel links. Therefore, we propose a scheme to select the user group that maximizes the effective channel capacity, by exhaustively searching the all the cases combined between N AUs and K users. We have termed this the effective channel capacity-based user group and beam selection scheme (ECC-UGBS).

First, it searches the RF beamforming matrix $\boldsymbol{\mathcal{W}}_F \in \mathbb{C}^{N_t\times(K\times N)}$ for $K \times N$ channel links. The RF beamforming vectors of kth user is

$$\left\{ \boldsymbol{w}_{i_{k,n}^*} \right\}_{n=1}^{N} = arg \max_{w_i \in W} \|\boldsymbol{H}_{k,n}\boldsymbol{w}_i\|^2. \tag{12}$$

Then, $\boldsymbol{\mathcal{W}}_F$ is given as

$$\boldsymbol{\mathcal{W}}_F = \left[\boldsymbol{w}_{i_{1,1}^*}, \ldots, \boldsymbol{w}_{i_{K,1}^*}, \boldsymbol{w}_{i_{1,2}^*}, \ldots, \boldsymbol{w}_{i_{K,N}^*}\right]. \tag{13}$$

Secondly, we form the user groups. Here, the number of users covered by each AU and user combinations are determined. For example, if $\mathrm{N} = 2, |K_1| = K, |K_2| = 0$, the number of user group set is 1. So, when the number of users covered by 1st AU and 2nd AU is $r_1 = 0,\ldots,K$ and $r_2 = K - r_1$, respectively, the number of all possible user group set is $N_S = K$. When N is 3, 4, or 5, the number of user group sets is $\sum_{m=1}^{K+1} m - N + 1$, $\sum_{M=1}^{K+1}\sum_{m=1}^{M} m - N + 1$, or $\sum_{M=1}^{K+1}\sum_{z=1}^{M}\sum_{m=1}^{z} m - N + 1$, respectively. A set of user groups can be expressed as $\mathbb{S} = [S(1), \ldots, S(N_S)]$, and user group subsets in each set are determined by user combinations.

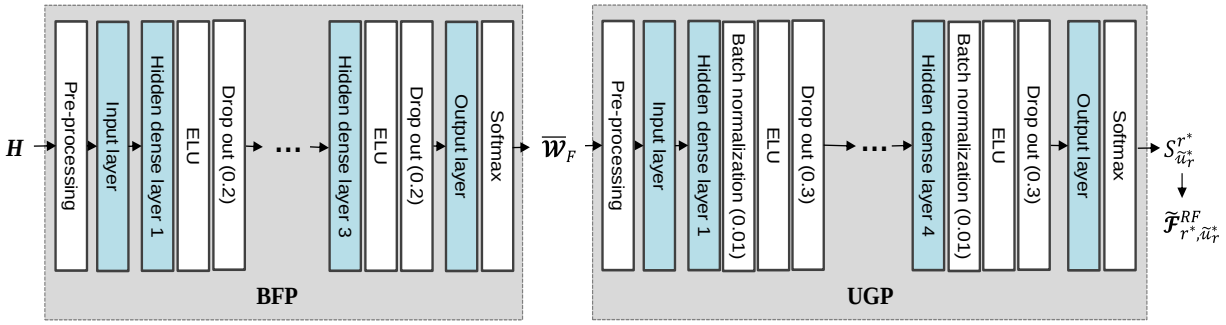

Figure 2. DNN model configuration for the proposed ML-ECC-UGBS.

The number of subsets in rth set is presented as $N_{S^r} = C_{r_1}^{K} \times C_{r_2}^{K-r_1} \times \cdots \times C_{r_{N-1}}^{K-(r_1+\cdots+r_{N-2})}$, $r = 1, \ldots, N_S - 1$, and $N_{S^{N_S}} = N$. Therefore, as the cell density increases, selecting the optimal user group becomes more complex.

Table 1 shows an example of user grouping when N = 2 and K = 5. The first and second columns represent sets and subsets, respectively. In set $S(3)$, r_1 and r_2 are 3 and 2, respectively. The third column represents the user combinations for each subset. There are C_5^3 subsets, $[S_1^3, S_2^3, \ldots, S_{10}^3]$, and the total number of subsets depends on N. $S_1^3 = \left[U_{1_1}, U_{2_1}, U_{3_1}, U_{4_2}, U_{5_2}\right]$ denotes that 1st, 2nd and 3rd users are connected to 1st AU, while 4th and 5th users are connected to 2nd AU. The channel matrix and beamforming matrix corresponding to gth user group subset S_g^r can be expressed as $\widetilde{\boldsymbol{H}}_{r,g} \in \mathbb{C}^{K \times N_t}$ and $\widetilde{\boldsymbol{\mathcal{F}}}_{r,g}^{RF}$ respectively, when arranged in the full channel matrix $\boldsymbol{H}$ and $\boldsymbol{\mathcal{W}}_F$. The effective channel $\overline{\boldsymbol{H}}_{r,g}$ of S_g^r is given by (10) and (11), and the effective channel capacity is

$$C\left(\overline{\boldsymbol{H}}_{r,g}, \rho\right) = \log_2 \det\left(\boldsymbol{I}_K + \rho \overline{\boldsymbol{H}}_{r,g} \overline{\boldsymbol{H}}_{r,g}^H\right). \tag{14}$$

The optimal user group is selected using

Table 1. User grouping example (N = 2, K = 5).

Set	Subset	Element of some subsets
$S(1)$	$[S_1^1, S_2^1, \ldots, S_5^1]$	$S_4^1 = \left[U_{4_1}, U_{1_2}, U_{2_2}, U_{3_2}, U_{5_2}\right]$
⋮	⋮	⋮
$S(3)$	$[S_1^3, S_2^3, \ldots, S_{10}^3$	$S_1^3 = \left[U_{1_1}, U_{2_1}, U_{3_1}, U_{4_2}, U_{5_2}\right]$
⋮	⋮	⋮
$S(5)$	$[S_1^0, S_2^0]$	$S_1^5 = \left[U_{1_2}, U_{2_2}, U_{3_2}, U_{4_2}, U_{5_2}\right]$ $S_2^5 = \left[U_{1_1}, U_{2_1}, U_{3_1}, U_{4_1}, U_{5_1}\right]$

$N_S = 5$, $\sum_{r=1}^{N_S} N_{S^r} = 32$.

$$\{r^*, g^*\} = arg \max_{\substack{r \in N_S \\ u \in N_{S^r}}} \left\{C\left(\overline{\boldsymbol{H}}_{r,g}, \rho\right)\right\}, \tag{15}$$

where g^*th user group of r^*th set is selected as the optimal user combination, which is used to determine the optimal RF beamforming matrix $\widetilde{\boldsymbol{\mathcal{F}}}_{r^*,g^*}^{RF}$.

4. Proposed ML-Based User Group and Beam Selection

For the conventional and ECC-UGBS schemes, the number of search iterations required to select optimal RF beams and covered users was $N \times K \times 2^{B_c}$ and $(N \times K \times 2^{B_c}) + \sum_{r=1}^{N_S} N_S{}^r$, respectively, as summarized in Table 2.

Simplifying beam selection and user scheduling is important in the case of increasingly dense and complex wireless networks. To accomplish this in coordinated multicell mmWave systems, we propose an ML-based ECC-UGBS (ML-ECC-UGBS), which includes processes that utilize the deep neural network (DNN) models for multiclass classification. ML-ECC-UGBS consists of the learning model for predicting the full beamforming matrix $\boldsymbol{\mathcal{W}}_F$ and the learning model for predicting the best user group. We have termed this DNN-based beamforming vector prediction (BFP) and user group prediction (UGP) models as shown in Fig. 2.

4.1 Training steps for BFP and UGP models

To design the BFP model, the correlation between the channel matrix and a selected RF beamforming vector is trained in the learning step, and the optimal vector is predicted in the test step. Training data, the complex channel samples and beamforming vector selected by (12), are gathered from a large set of randomly deployed AUs and users. The complex channel vectors are separated into their real and imaginary components since DNNs cannot learn complex numbers. The jth channel sample $\boldsymbol{H}_{k,n}^{(j)}$ can be represented as the training data $\boldsymbol{R}_j^B \in \boldsymbol{R}_B$ as follows:

$$\boldsymbol{R}_j^B = \left[\Re\left\{h_{k,n,1}^{(j)}\right\}, \Im\left\{h_{k,n,1}^{(j)}\right\}, \dots, \Re\left\{h_{k,n,N_t}^{(j)}\right\}, \Im\left\{h_{k,n,N_t}^{(j)}\right\}\right], \tag{16}$$

Table 2. Scheme comparison.

Scheme	Number of search iterations required	
	RF beam	User group
Conventional	$N \times K \times 2^{B_c}$	
ECC-UGBS	$N \times K \times 2^{B_c}$	$\sum_{r=1}^{N_S} N_S{}^r$

where $h_{k,n,i}^{(j)}$ is the ith element of $\boldsymbol{H}_{k,n}^{(j)}$, $i = 1, \dots, N_t$, and $j = 1, \dots, L_B$, and L_B is the number of gathered channel samples. Notably, the mmWave channel impulse response is significantly impacted by the frequency selective fading and the line-of-sight and non-line-of-sight characteristics of the propagation path, so accurate learning requires normalization. The entire training data $\boldsymbol{R}_B \in \mathbb{C}^{L_B \times 2N_t}$ is normalized as:

$$\bar{\boldsymbol{R}}_B = \frac{\boldsymbol{R}_B - \min_{j \in L_B}\left(\boldsymbol{R}_j^B\right)}{\max_{j \in L_B}\left(\boldsymbol{R}_j^B\right) - \min_{j \in L_B}\left(\boldsymbol{R}_j^B\right)}. \tag{17}$$

For each training data $\bar{\boldsymbol{R}}_j^B$, the beamforming vector index $i_k^{(j)*}$ given by $i_k^{(j)*} = arg \max_{w_i \in W} \left\| \boldsymbol{H}_{k,n}^{(j)} \boldsymbol{w}_i \right\|^2$ is encoded by the one-hot encoding scheme and used as a class label.

For the UGP model, we conducted DNN training tests using diverse data, such as channel matrices, beamforming matrices, and effective channel matrix to determine the optimal training data type. Consequently, the RF beamforming information was derived as the most optimal training data type via simulation tests. The

RF beamforming vector expression can be simplified using (8) and (9) in comparison with the mmWave channel. Further, because (12) yields a beamforming vector similar to the channel, it is considered to represent the channel. Therefore, the correlation between RF beamforming matrix and selected user group was trained to enable prediction of a user group to maximize effective channel capacity. In this regard, two models are investigated using different data types for UGP. The input data of UGP model 1 is the RF beamforming matrix and the input data of UGP model 2 is the indices of the RF beamforming vectors. To gather the training data, N AUs and K users were deployed L_U times in the system and the network environment described in Section II. For UGP model 1, the RF beamforming vector $\overline{\boldsymbol{W}}_F^{(j)} \in \mathbb{C}^{1\times(N_t\times K\times N)}$ for $K \times N$ channel link is obtained from (12) and (13), $j = 1, \dots, L_U$. This is expressed as $\overline{\boldsymbol{W}}_F^{(j)} = \left[\boldsymbol{w}_{i_{1,1}^*}^{(j)^T}, \dots, \boldsymbol{w}_{i_{K,N}^*}^{(j)^T}\right]$. $\overline{\boldsymbol{W}}_F^{(j)}$ is converted to R_j^F as (16), and $\overline{\boldsymbol{R}}_F \in \mathbb{C}^{L_U\times(2N_t\times K\times N)}$ is given by (17). For UGP model 2, $\overline{\boldsymbol{W}}_\jmath^{(j)} \in \mathbb{C}^{1\times(K\times N)}$ from $\left\{ i_{k,n}^{(j)*} \right\}_{n=1}^{N} = arg \max_{w_i\in W} \left\| \boldsymbol{H}_{k,n}^{(j)} \boldsymbol{w}_i \right\|^2$ is obtained, and it is expressed as $\overline{\boldsymbol{W}}_\jmath^{(j)} = \left[i_{1,1}^{(j)*}, \dots, i_{K,N}^{(j)*}\right]$. $\overline{\boldsymbol{R}}_\jmath \in \mathbb{C}^{L_U\times(K\times N)}$ is given by (17).

There are two ways to train the UGP model. The first is to bundle the entire set $\widehat{\mathbb{S}} = \left[\mathbb{S}^{(1)}, \dots, \mathbb{S}^{(j)}, \dots, \mathbb{S}^{(L_U)}\right]$ into one training data set to be learned, where $\mathbb{S}^{(j)} = \left[S^{(j)}(1), \dots, S^{(j)}(N_S)\right]$, and r^* and u^* are predicted as outputs. However, the UGP model trained for K users and N AUs network is difficult to apply it for $\acute{K}$ users and $\acute{N}$ AUs network because the length of training data depends on K and N. For example, the previous work [15] found that the number of users that could be optimally covered by one AU was limited, set as $\hat{K}$. Here, when the users covered by an AU are already $\hat{k}$, the users to be covered and combinations for $\hat{K} - \hat{k}$ users must be newly determined in that AU. Furthermore, the UGP model trained in this manner is not appropriate in several cases, including predicting only a combination of users or adding a new subset combination, which require new training data and labels to be set and relearned each time. The UGP model in the first way must be set and relearned with new training data and labels according to changes in conditions such as adding a new subset combination. Thus, we propose a second training option for the UGP model based on a modular concept. Modules are distinguished by the number of covered users, so the number of modules is $N_M = N_S$. In the UGP model, indices of user groups of each set are used as a label for modules. The effective channel matrix of $\hat{r}$th set $S^{(j)}(\hat{r}) \in \mathbb{S}^{(j)}$ of the jth channel sample is

$$\overline{\boldsymbol{H}}_{\hat{r}}^{(j)} = \left[\overline{\boldsymbol{H}}_{\hat{r},1}^{(j)}, \dots, \overline{\boldsymbol{H}}_{\hat{r},u}^{(j)}, \dots, \overline{\boldsymbol{H}}_{\hat{r},N_{S^r}}^{(j)}\right], \hat{r} = 1, \dots, N_M, \tag{18}$$

with the capacity of $\overline{\boldsymbol{H}}_{\hat{r},u}^{(j)}$ given by (14). The index of the optimal user group of set $S^{(j)}(\hat{r})$ is

$$\left\{u_{\hat{r}}^{(j)*}\right\} = arg \max_{u\in N_{S^{\hat{r}}}} \left\{ C\left(\overline{\boldsymbol{H}}_{\hat{r},u}^{(j)}, \rho\right)\right\}. \tag{19}$$

Therefore, the indices for the $\hat{r}$th module are

$$\overline{\boldsymbol{u}}_{\hat{r}} = \left[u_{\hat{r}}^{(1)*}, \dots, u_{\hat{r}}^{(j)*}, \dots, u_{\hat{r}}^{(L_U)*}\right]^T, \tag{20}$$

where $\overline{\boldsymbol{u}}_{\hat{r}}$ is encoded by the one-hot encoding scheme. For the $\hat{r}$th module, $\overline{\boldsymbol{R}}_F, \overline{\boldsymbol{R}}_\jmath$ and encoded $\overline{\boldsymbol{u}}_{\hat{r}}$ are used to train a DNN, and other DNNs of N_M modules are trained similarly.

4.2 Test and operation steps for BFP and UGP models

BFP and UGP models are trained on prepared data in the training steps, and their DNNs are optimized. In our proposed system, the trained BFP and UGP models are equipped at the CU. When users request service, the entire channel H is transformed by (16) and (17) and input to the BFP, and $\overline{\boldsymbol{W}}_F$ is predicted. The $\overline{\boldsymbol{W}}_F$ transformed by (16) and (17) is then input to the UGP with N_M modules, which predict the user group indices

as $[\tilde{u}_1, \ldots, \tilde{u}_{N_M}]$. An optimal user group $S^{r^*}_{\tilde{u}^*_r}$ is selected among subsets of indices $[\tilde{u}_1, \ldots, \tilde{u}_{N_M}]$ by (15). Then, the optimal RF beamforming matrix $\tilde{\mathcal{F}}^{RF}_{r^*,\tilde{u}^*_r}$ is determined.

5. Numerical Results and Discussion

Herein, we evaluate the proposed scheme based on a coordinated multicell mmWave system. The performance is evaluated for spectral efficiency, computation time, and computational complexity.

5.1 Building the neural networks

We have applied an optimized DNN architecture, derived from numerous experiments, to design BFP and UGP models. The DNN compositions for both models are as follows. The DNN for BFP contained 3 dense hidden layers (HLs) with 64 neurons, exponential linear units (ELU) activation, 0.2 dropout layers (DL) per HL, an Adam optimizer, softmax activation in the output layer (OL), and the categorical cross-entropy (CCE) as a loss function in the compiler. The DNNs for UGP model 1 contained of 4 HLs with 384 neurons, ELU, 0.3 DL, 0.01 batch normalization per HL, Adam, softmax, and CCE. The DNNs for UGP model 2 contained of 4 HLs with 64 neurons, ELU, 0.02 DL per HL, Adam, softmax, and CCE.

5.2 System setup and simulation parameters

The proposed system was designed in MATLAB® and Python. The Keras tool with a TensorFlow backend engine was used to design the DNNs on a computer with an Intel® Core™ i7-8700 3.20 GHz, an NVIDIA GeForce RTX 2070, and 16 GB of memory. A carrier frequency of 28 GHz was used. Two small cells with a 30 m radius were simulated. The separation distance between AUs in small cells was 40 m, and five users were randomly deployed in the overlapped area, which was 613.8 m2. Each AU was equipped with a 4×4 uniform rectangular array ($N_t = 16, N_v = 4, N_h = 4$). The B_c, L_B, and L_U used were 10, 100,000, and 200,000, respectively.

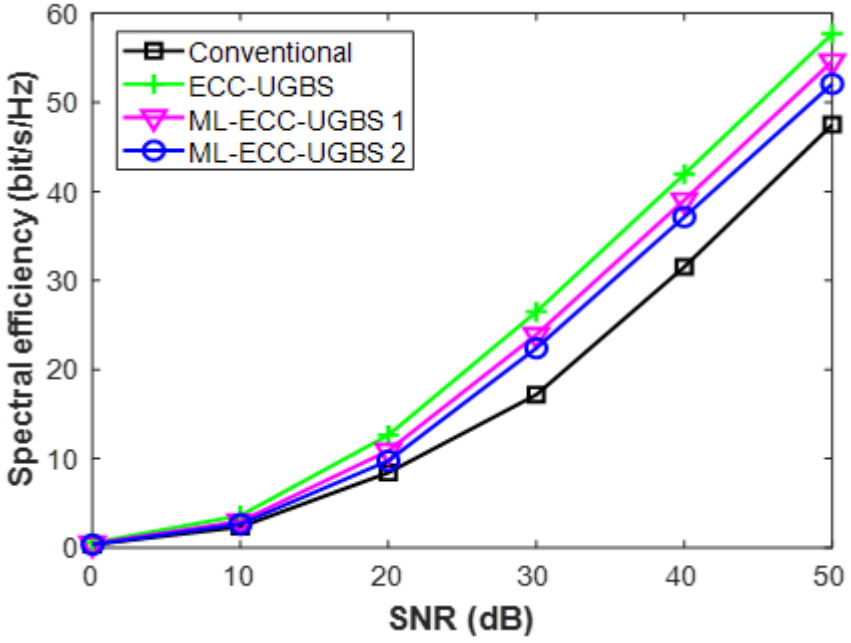

Figure 3. Spectral efficiency of conventional and proposed schemes versus SNR.

5.3 Performance evaluation

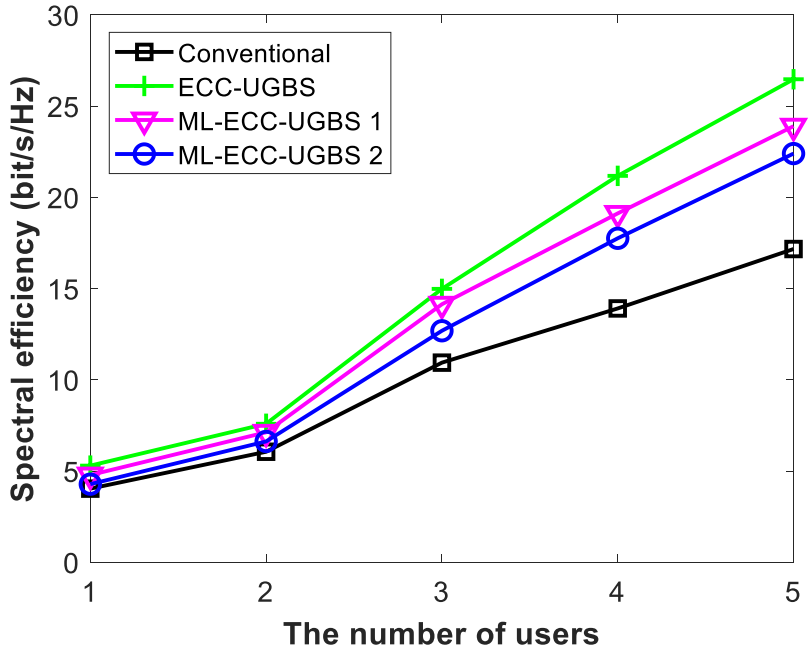

Figure 4. Spectral efficiency of conventional and proposed schemes versus the number of users (for SNR= 30 dB).

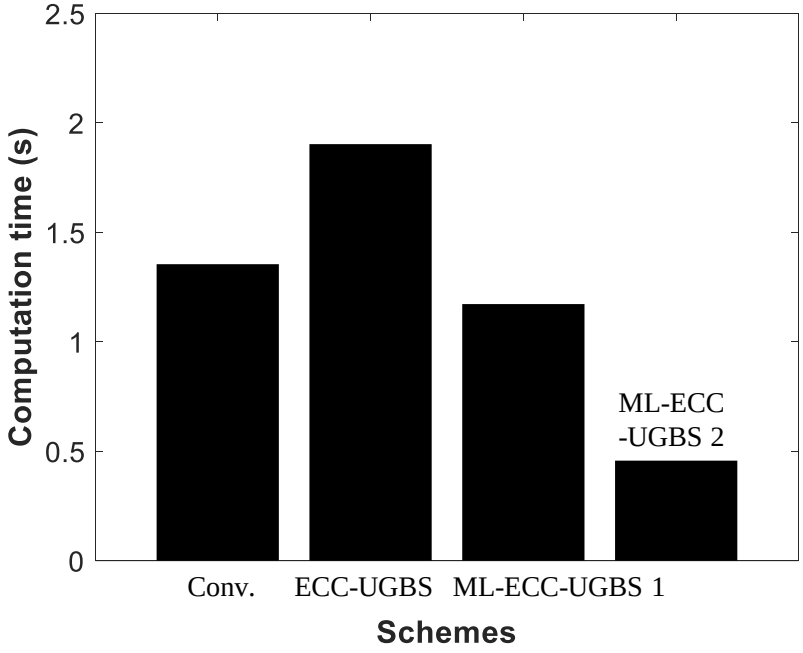

Figure 5. Computation time for conventional and proposed schemes.

Spectral efficiency, as calculated by (5), is shown in Fig. 3 and Fig. 4 for the proposed ML-ECC-UGBS 1, 2 and ECC-UGBS compared to the conventional scheme, where ML-ECC-UGBS 1 and 2 are based on UGP model 1, and 2, respectively. The best performance is achieved by the ECC-UGBS based on an exhaustive user group search. The ML-ECC-UGBS 1 and 2 achieved similar, near-optimal performance, but were affected by prediction errors. The training data length of ML-ECC-UGBS 2 is $1/2N_t$ of ML- ECC-UGBS 1, and their performance difference is about 3~4%. While the conventional scheme and similar approaches are widely used in current systems with downlink pilots, such as 4G or primary 5G, these schemes exhibit inferior performance compared to those proposed here. In Fig. 4, it was analyzed that the performance gap increased as the number of users increased. This implies that the proposed schemes effectively mitigate ICI. In Fig. 5, the computation time required to determine the optimal beamforming matrix and user group is compared for a 5G new radio subframe with 125 resource blocks, or channels. Here, the ML-ECC-UGBS 2 has a significantly lower computation time, 0.457 s, than either ECC-UGBS, ML-ECC-UGBS 1 or conventional schemes, which required 1.903 s, 1.172 s and 1.354 s, respectively. Notably, the results in Fig. 3 depend on the search iterations required as summarized in Table II and the length of training data.

5.4 Analysis of computational complexity

Then, the computational complexity of the conventional and proposed schemes is compared. We consider the complexity of the prediction phase of ML based schemes because the training phase can be performed online. Since the best beam and the serving cell are selected by using (7) for $N \times K \times 2^{B_c}$ times in the conventional scheme, the complexity is

$$\boldsymbol{\mathcal{O}}(2^{B_c}NK(2N_t+3)). \tag{21}$$

The proposed ECC-UGBS selects the optimal user group after grouping users and selecting all beams, so the complexity is

$$\boldsymbol{\mathcal{O}}\left(2^{B_c}NK(2N_t+3)+\sum_{r=1}^{N_S}N_S{}^r\left(KN_t^2+N_t\left(K-\frac{N_t}{2}\right)-\frac{N_t}{2}+2K^2+\frac{2}{3}K^3\right)\right). \tag{22}$$

The proposed ML-ECC-UGBS 1 and 2 consist of BFP and UGP models. When N_{I_1}, n_1, D_{r_1}, and N_{H_1} present the length of input test data, the neuron numbers of HLs, dropout rate, and the number of HLs, respectively, for the DNN of a BFP model, the complexity for the beam prediction is $\boldsymbol{\mathcal{O}}\left(N_{I_1}n_1+(N_{H_1}-1)\left(1-d_{r_1}\right)n_1^2+2^{B_c}n_1\left(1-d_{r_1}\right)\right)$. For DNNs of a UGP model, N_{I_2}, n_2, D_{r_2}, and N_{H_2} present the length of input test data, the neuron numbers of HLs, dropout rate, and the number of HLs, respectively. The complexity for best user group prediction is $\boldsymbol{\mathcal{O}}\left(N_{I_2}n_2+(N_{H_2}-1)\left(1-d_{r_2}\right)n_2^2+\sum_{r=1}^{N_S}N_S{}^r\,n_2\left(1-d_{r_1}\right)\right)$. Thus, the complexity for ML-ECC-UGBS 1 and 2 are

$$\boldsymbol{\mathcal{O}}\left(N_{I_1}n_1+(N_{H_1}-1)\left(1-d_{r_1}\right)n_1^2+2^{B_c}n_1\left(1-d_{r_1}\right)+N_{I_2}n_2+(N_{H_2}-1)\left(1-d_{r_2}\right)n_2^2+\sum_{r=1}^{N_S}N_S{}^r\,n_2\left(1-d_{r_1}\right)\right). \tag{23}$$

6. Conclusion

In this work, we investigated user group and beam selection schemes to maximize spectral efficiency and mitigate ICI for coordinated multicell mmWave systems. The proposed scheme achieves better performance than conventional schemes, for both spectral efficiency and computation time. The simulation results demonstrate that the proposed scheme reduces network latency while increasing data rates and can be utilized

to satisfy requirements of advanced MWCs. In the future, novel schemes using advanced neural networks could be studied for the large-scale mmWave systems in more complex and dense network environments.

Acknowledgement

This work was supported by an Institute for Information & Communications Technology Promotion (IITP) grant funded by the Korean Government (MSIT) (Grant No. 2016-0-00183).

This work was financially supported by the Research Year of Chungbuk National University in 2020.

References

[1] Ericsson: “Ericsson mobility report (Revision A),” 2019.

[2] R. W. Heath, N. G.-Prelcic, S. Rangan, W. Roh, A. M. Sayeed, "An overview of signal processing techniques for millimeter wave MIMO systems," *IEEE J. Sel. Topics Signal Process*., vol. 10, no. 3, pp. 436–453, April 2016. doi: 10.1109/JSTSP.2016.2523924.

[3] D. L.-Pérez, M. Ding, H. Claussen, and A. H. Jafari, "Towards 1 Gbps/UE in cellular systems: Understanding ultra-dense small cell deployments," *IEEE Commu. Surv. Tuts*., vol. 17, no. 4, pp. 2078-2101, 2015. doi: 10.1109/COMST.2015.2439636.

[4] M. Kamel, W. Hamouda, and A. Youssef, "Ultra-dense networks: A survey," *IEEE Commu. Surv. Tuts.*, vol. 18, no. 4, pp. 2522–2545, 2016. doi: 10.1109/COMST.2016.2571730.

[5] A. Alkhateeb, G. Leus, and R. W. Heath, "Limited feedback hybrid precoding for multi-user millimeter wave systems," *IEEE Trans. Wirel. Commun.*, vol. 14, no. 11, pp. 6481-6494, Nov. 2015. doi: 10.1109/TWC.2015.2455980.

[6] Z. Jiang, S. Chen, S. Zhou, and Z. Niu, “Joint user scheduling and beam selection optimization for beam-based massive MIMO downlinks,” *IEEE Trans. Wirel. Commun*., pp. 2190-2204, April 2018. doi: 10.1109/TWC.2018.2789895.

[7] S. He, Y. Wu, D. W. K. Ng, and Y. Huang, “Joint optimization of analog beam and user scheduling for millimeter wave communications,” *IEEE Commun. Lett*., vol. 21, no. 12, pp. 2638-2641, Dec. 2017. doi: 10.1109/LCOMM.2017.2745570.

[8] M. A.-Saedy, M. A.-Imari, M. A.-Shuraifi, and H. A.-Raweshidy, “Joint user selection and multimode scheduling in multicell MIMO cellular networks,” *IEEE Trans. Veh. Technol*., vol. 66, no. 12, pp. 10962-10972, Dec. 2017. doi: 10.1109/TVT.2017.2717909.

[9] R. P. Antonioli, G. Fodor, P. Soldati and T. F. Maciel, "User Scheduling for Sum-Rate Maximization Under Minimum Rate Constraints for the MIMO IBC," *IEEE Wirel. Commun. Lett.*, vol. 8, no. 6, pp. 1591-1595, Dec. 2019, doi: 10.1109/LWC.2019.2930255.

[10] İ. Cumali, B. Özbek and A. Pyattaev, "Beam and User Selection Technique in Millimeter Wave Communications," *2020 IEEE 91st Vehicular Technology Conference (VTC2020-Spring)*, Antwerp, Belgium, 2020, pp. 1-5, doi: 10.1109/VTC2020-Spring48590.2020.9128737.

[11] Y. Long, Z. Chen, J. Fang, and C. Tellambura, “Data-Driven-Based Analog Beam Selection for Hybrid Beamforming Under mm-Wave Channels,” *IEEE J. Sel. Topics Signal Process*., vol. 12, no. 2, pp. 340–352, March 2018. doi: 10.1109/JSTSP.2018.2818649.

[12] Y. Yang, X. Deng, D. He, Y. You, and R. Song, “Machine Learning Inspired Codeword Selection for Dual Connectivity in 5G User-Centric Ultra-Dense Networks,” *IEEE Trans. Veh. Technol*., vol. 68, no. 8, pp. 8284-8288, June. 2019. doi: 10.1109/TVT.2019.2923314.

[13] 3GPP, “Study on channel model for frequencies from 0.5 to 100 GHz (Release 14),” 3GPP, Tech. Rep. TR38.901, V14.3.0, 2017.

[14] B. M. Hochwald, T. L. Mazetta, T. J. Richardson, W. Sweldens, and R. Urbanke, “Systematic design of unitary space-time constellations,” *IEEE Trans. Inform. Theory*, vol. 46, no. 6, pp. 1962-1973, Sep. 2000. doi: 10.1109/18.868472.

[15] S.-L. Ju, N.-il Kim, S.-Q. Lee, J. Kim, and K.-S. Kim, "Hybrid beamforming scheme for millimeter-wave massive MIMO and dense small cell networks," *25th Asia-Pacific Conference on Communications*, 2019.